

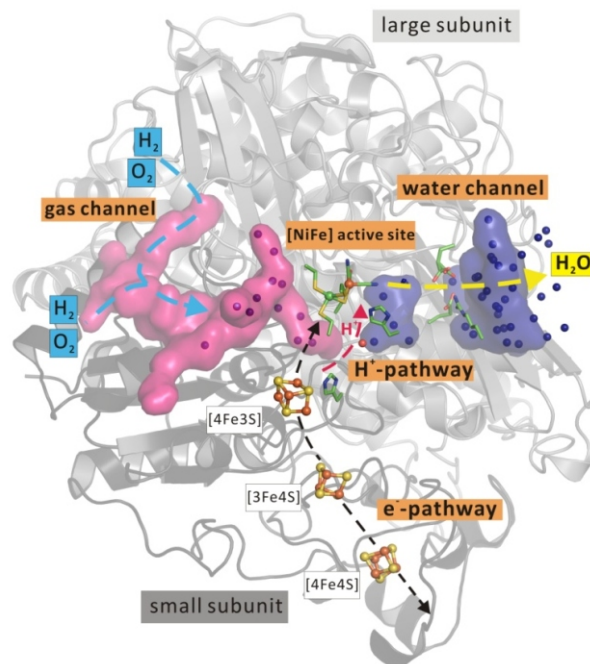
**Posters - Theory and Practice of Crystallization**

P12-1

**THE FINE-TUNED MACHINERY OF O<sub>2</sub>-TOLERANT [NiFe] HYDROGENASE**
**Andrea Schmidt, Jacqueline Kalms and Patrick Scheerer\***
*Institut für Medizinische Physik und Biophysik (CC2), Group Protein X-ray Crystallography & Signal Transduction, Charité - Universitätsmedizin Berlin, Charitéplatz 1, D-10117 Berlin, Germany*
*\*patrick.scheerer@charite.de*

Hydrogenases are metalloenzymes catalyzing the heterolytic splitting of hydrogen into protons and electrons. In all three domains of life hydrogenases are domiciled, but only a small subgroup of [NiFe] hydrogenases evolved the feature of hydrogen conversion under aerobic conditions. For enabling the aerobic hydrogen oxidation in [NiFe] hydrogenases, multiple adaptable pathways have been evolved. Structural investigations on this biological machine might lead to new developments in the field of renewable energy technologies [1].

The membrane-bound [NiFe] hydrogenase (MBH) of *Ralstonia eutropha* (*R.e.*) is one of the best investigated typical O<sub>2</sub>-tolerant hydrogenases. Several crystal structures of the MBH *R.e.* as wildtype or with multiple substitutions in different redox states reveal a highly fine-tuned interplay between pathways and channels that lead to a perfect transport of reagents and products to and from the active site [2, 3]. For hydrogen splitting the [NiFe] active site of MBH *R.e.* requires the delivery of hydrogen via a hydrophobic gas channel. Hydrogen oxidation liberates electrons which are guided via an electron pathway to an electron acceptor. Subsequently, the electrons enter the quinone pool of the respiratory chain as reduction power for the cell [2]. Under aerobic conditions additionally the [NiFe] active site has to reduce the attacking oxygen to water with 4 e<sup>-</sup> and 4 H<sup>+</sup>. On that account the electron pathway, consisting of three [FeS] clusters, has to operate bidirectional. A unique [4Fe-3S] cluster proximal to the active site is mainly involved in this switch. This [4Fe-3S] cluster undergoes redox-dependent reversible transformations, namely iron-swapping between a sulfide and a peptide amide N. For proton delivery several pathways close to the active site have been investigated and introduce new questions that might be answered by investigative methods e.g. neutron diffraction. The gas channel that is supplying also the inhibitory oxygen has been adapted especially in quantity and size to remain the hydrogenase activity for the system [4]. Water molecules produced under oxygen reduction are released through a new water channel. This complex system is still not completely understood and moreover sensitive to X-rays. Consequently a near radiation-damage free technique, the free-electron laser (e.g. LCLS, Stanford, USA), has been used to gain further insights into the functionality of this enzyme.



1. Fritsch, J., Lenz, O., Friedrich, B. (2013). Structure, function and biosynthesis of O<sub>2</sub>-tolerant hydrogenases. *NatRevMicrobiol.* **2**, 106-114.
2. Fritsch, J., Scheerer, P., Frielingsdorf, S., Kroschinsky, S., Friedrich, B., Lenz, O., Spahn, CM. (2011). The crystal structure of an oxygen-tolerant hydrogenase uncovers a novel iron-sulfur centre. *Nature* **479** (7372), 249-52.
3. Frielingsdorf S, Fritsch J, Schmidt A, Hammer M, Löwenstein J, Siebert E, Pelmenschikov V, Jaenicke T, Kalms J, Rippers Y, Lenzian F, Zebger I, Teutloff C, Kaupp M, Bittl R, Hildebrandt P, Friedrich B, Lenz O<sup>S</sup>, and Scheerer P<sup>S</sup>. (2014). Reversible [4Fe-3S] cluster morphing in an O(2)-tolerant [NiFe] hydrogenase. *Nat Chem Biol.* **10**, 378-385.
4. Kalms, J., Schmidt, A., Frielingsdorf, S., van der Linden, P., von Stetten, D., Lenz, O., Carpentier, P., Scheerer, P. Gas transport through a hydrophobic tunnel in O<sub>2</sub>-tolerant membrane-bound [NiFe] hydrogenase from *Ralstonia eutropha*. *Angew Chem Int Ed Engl.* 2016, doi: 10.1002/anie.201508976.



P12-2

## DECIPHERING THE STRUCTURAL AND FUNCTIONAL ASPECTS OF GGEEF PROTEIN DOMAIN INVOLVED IN LIFESTYLE SWITCH OF *VIBRIO CHOLERAE*

D. Bandekar and S. Biswas

VISTA Lab, Department of Biological Sciences, BITS Pilani, KK Birla, Goa Campus, Zuarinagar, Goa 403726, p2012008@goa.bits-pilani.ac.in

The Gram negative flagellate *Vibrio cholerae* survives between cholera epidemics as surface biofilms in aquatic bodies. These surface biofilms are resistant to external stress like antibiotics, chlorine, predators and other factors. Proteins with GGEEF domain have diguanylate cyclase activity which modulates the intracellular level of bis-(3'-5')-cyclic dimeric guanosine monophosphate (c-di-GMP) which, in turn, regulates the switch between the motile and planktonic form of the pathogen. VC0395\_0300 is a putative protein from *Vibrio cholerae* that has the GGEEF domain which shows promising biofilm forming capability. Constructs of the gene-of-interest were created to provide structural and functional insights into the role of the GGEEF domain in biofilm formation. The structure was modeled by using closest structural homolog template and maximum sequence alignment. Comparison with available crystal structures of the GGEEF domain depicted the presence of a central sheet and five helices. This is supported by secondary structure prediction which shows 41.43% helix, 23.36% strand and 35.20% loops in the protein structure.

The presence of tryptophan residues (W4 and W172) in the proteins has enabled us to monitor tryptophan fluores-

cence by thermal and chemically induced unfolding. From the fluorescence quenching studies with acrylamide, KI and CsCl on native and denatured protein, we could determine that one of the tryptophans resides in a positively charged pocket. Furthermore, transverse urea gradient gel (TUGE) reinforces the fact that the protein shows two-state (native and unfolded) unfolding transition. Likewise, size exclusion chromatography and glutaraldehyde cross-linking have highlighted the oligomerization tendency of the protein. To gather more information on the crystal structure, crystallization trials were attempted in various screens and the work is in progress.

1. B.K. Hammer, B.L. Bassler, *J. Bacteriol.*, **91**, (2009), 169-177.
2. D. A. Ryjenkov, M. Tarutina, O. V. Moskvina, M. Gomelsky, *J. Bacteriol.*, **187**, (2005), 1792-1798.

*The authors would like to acknowledge BRNS, DAE for funding the research project and for providing fellowship to DB.*

P12-3

## STRUCTURAL COMPARISON OF PUTATIVE ALANINE RACEMASES Alr AND YlmE FROM *STREPTOMYCES COELICOLOR* A3(2)

R. Tassoni<sup>1</sup>, L. van der Aart<sup>2</sup>, M. Ubbink<sup>1</sup>, G. P. van Wezel<sup>2</sup>, N. S. Pannu<sup>1\*</sup>

<sup>1</sup>Leiden Institute of Chemistry, Leiden University, Gorlaeus Laboratories, Einsteinweg 55, 2333 CC Leiden, The Netherlands

<sup>2</sup>Institute of Biology Leiden, Leiden University, Sylviusweg 72, 2333 BE Leiden, The Netherlands  
\*raj@chem.leidenuniv.nl

The conversion of L-alanine into D-alanine in bacteria is essential for cell wall synthesis and bacterial survival, and performed by pyridoxal phosphate (PLP)-dependent enzymes called alanine racemases. Based on sequence annotation, the two genes *alr* and *ylmE* of *Streptomyces coelicolor* A3(2) are hypothesised to encode for proteins with alanine racemase activity. In the present study, we present the crystallization and crystal structures of both uncomplexed Alr and YlmE and in complex with ligands. The two proteins share a common  $\alpha/\beta$  barrel fold, which characterizes the N-terminal domain of Alr and the whole YlmE peptide. In both proteins, the catalytic PLP-cofactor is bound to a lysine residue located in the core of the  $\alpha/\beta$  barrel domain, Lys46 in Alr and Lys40 in YlmE. Despite

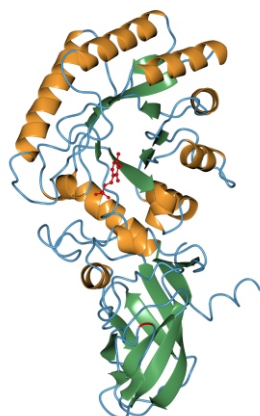


**Figure 1.** A ribbon representation of the Alr monomer.  $\alpha$ -Helices and  $\beta$ -strands are represented in orange and green, respectively. The PLP cofactor is shown as a ball-and-stick model in red. The catalytic Tyr283 is highlighted in red.

these common features, YlmE lacks the C-terminal domain present in Alr and that mediates homodimerization by head-to-tail binding with the N-terminal domain. Furthermore, *in vitro* biochemical studies show alanine racemization only for Alr, with a rate of  $2.12 \mu\text{mol min}^{-1}$  for the racemization of L- to D-Ala and  $2.90 \mu\text{mol min}^{-1}$  for the opposite direction. Our results confirm the alanine racemase activity of Alr and open the way for further studies to elucidate the function of YlmE.

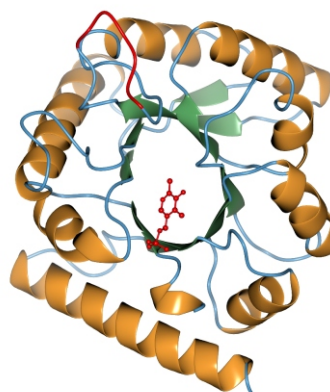


**Figure 2.** A ribbon representation of the YlmE fold.  $\alpha$ -Helices and  $\beta$ -strands are represented in orange and green, respectively. The PLP cofactor is shown as a ball-and-stick model in red. The residues highlighted in red correspond to a flexible loop region.

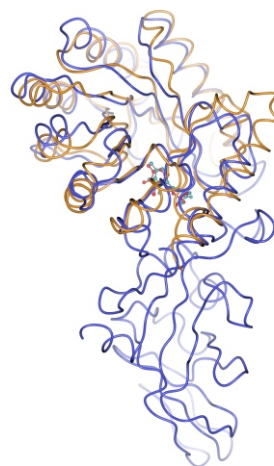


**Figure 3.** Superposition of Alr (blue) and YlmE (orange). The PLP cofactors are shown as ball-and-stick models and are coloured in dark cyan and red for Alr and YlmE, respectively. YlmE superposes well with the N-terminal domain of Alr but lacks the C-terminal domain responsible for dimerization and alanine racemization activity.



P12-4

## CRYSTALLIZATION AND STRUCTURE SOLUTION OF PHOSPHOLIPASEACYLTRANSFERASE IN COMPLEX WITH POTENT INHIBITORS

K.C. Zwiers, S. Chatterjee, P. Voskamp, J. Zhou, K. Al Ayed, B. Narhe, M. Ubbink, M. van der Stelt, N.S. Pannu

Gorlaeus Laboratories, Leiden institute of Chemistry, Leiden University, The Netherlands.  
k.c.zwiers@umail.leidenuniv.nl

Over one third of adults in America are obese and thus are at risk on type 2 diabetes, cancer and cardiovascular diseases. Phospholipase-Acyltransferase (PLA/AT) are important enzymes that are crucial in the development of obesity. We have recently designed a class of reversible PLA/AT inhibitors showing micromolar inhibition that are promising candidate anti-cancer or anti-obese drugs. The crystal structure of PLA1/AT3 and PLA2/AT3 have been reported [1], but the binding pocket is very large and consequently the inhibitors may have multiple binding modes. Here, we describe the crystallization and preliminary structure analysis of PLA/AT soaked with various inhibitors. Soaking PLA/AT protein crystals with inhibitors remains challenging, as the designed inhibitors are poorly soluble. Our re-

sults demonstrate that it was possible to obtain inhibitor soaked non-damaged crystals for PLA/AT 2, by varying the concentrations of inhibitor and various solubilizing agents, cryo protectant and protein crystal buffer solution. The resulting crystals were collected and resulted in high-resolution datasets of 1.4 Å, respectively. We will optimize these results in future co-crystallization experiments or for the improvement of soaking other PLA/AT family members (1, 3-5) with a wide variety of inhibitors.

1. M. Golczak, A. E. Sears, P. D. Kiser, and K. Palczewski, LRAT-specific domain facilitates vitamin A metabolism by domain swapping in HRASLS3, Nat. Chem. Biol., vol. 11, no. 1, pp. 26-32, Jan. 2015.

P12-5

## THIOSULFATE DEHYDROGENASE (TsdA) FROM *ALLOCHROMATIUM VINOSUM*: STRUCTURAL AND FUNCTIONAL INSIGHTS INTO THIOSULFATE OXIDATION

José A. Brito<sup>1</sup>, Kevin Denkmann<sup>2</sup>, Inês A. C. Pereira<sup>1</sup>, Christiane Dahl<sup>2</sup> & Margarida Archer<sup>1</sup>

<sup>1</sup>Instituto de Tecnologia Química e Biológica – António Xavier, Universidade Nova de Lisboa, Av. República, 2780-157 Oeiras, Portugal

<sup>2</sup>Institut für Mikrobiologie & Biotechnologie, Rheinische Friedrich-Wilhelms-Universität Bonn, Meckenheimer Allee 168, D-53115 Bonn, Germany  
archer@itqb.unl.pt and chdahl@uni-bonn.ed

The ability to perform the very simple oxidation of two molecules of thiosulphate to tetrathionate is wide spread among prokaryotes. Despite the widespread occurrence of tetrathionate formation, and its well-documented significance within the sulphur cycle, little is known about the enzymes catalysing the oxidative condensation of two thiosulphate anions. To fill this gap, the thiosulphate dehydrogenase (TsdA), enzyme from *Allochromatium vinosum*, was recombinantly expressed, purified and kinetic and spectroscopically characterized [1]. Moreover, we solved the crystal structure of the enzyme by Single Anomalous Dispersion (SAD) method using the Fe-haem anomalous signal. We have further obtained X-ray structures of TsdA in several redox states.

The protein crystallized in space group C2 with PEG 3350 as precipitant and one molecule in the asymmetric unit [2]. Initial crystallization trials rendered multiple, urchin-like crystals with no diffraction ability. Using iodide as an additive worked as a “silver bullet” allowing to obtain single crystals that diffract to 1.4Å resolution. TsdA contains two typical class I c-type cytochrome domains with

two hemes axially coordinated by His53/Cys96 and His164/Lys208. The X-ray structure showed an all-alpha structure with structural similarities to the *Rhodovulum sulfidophilum*'s SoxAX (PDB code 2OZ1), and the low-redox-potential cytochrome c6 from *Hizikia fusiformis* (PDB code 2ZBO).

Interestingly, reduction of the enzyme causes a ligand switch from Lys208 to Met209 in heme 2. TsdALys208 Asn or Lys208Gly variants exhibit similar substrate affinities as the wildtype protein but much lower specific activities pointing at this heme as the electron exit point. Cys96 is essential for catalysis. Overall, our kinetic, spectroscopic and structural data lead us to propose a mechanism where two thiosulfate molecules enter the active site, inducing a movement of the S of Cys96 out of the iron coordination sphere; this ligand movement results in an increase of the redox potential of heme 1, thus allowing the sequential uptake of the two electrons resulting from the conversion of the two thiosulfates to tetrathionate, leading to the reduction of both hemes; upon reduction, heme 2 undergoes a ligand switch, which increases its redox potential and hin-

ders the back reaction. Most likely, HiPIP serves as the electron acceptor *in vivo*.

1. Denkmann K., Grein F., Zigann R., Siemen A., Bergmann J., van Helmont S., Nicolai A., Pereira I. A. C., Dahl C. (2012) Thiosulfate dehydrogenase: a widespread unusual acidophilic *c*-type cytochrome. *Environ. Microbiol.* **14**(10):2673-2688.
2. Brito, J. A., Guiterres, A., Denkmann, K., Pereira, I. A. C., Dahl, C., and Archer, M.. (2014) Production, crystalliza-

tion and preliminary crystallographic analysis of *Allochromatium vinosum* TsdA, an unusual acidophilic *c*-type cytochrome. *Acta Cryst.* **F70**:1424-1427.

3. Brito, J. A., Denkmann, K., Pereira, I. A. C., Archer, M., and Dahl, C.. (2014) Thiosulfate Dehydrogenase (TsdA) from *Allochromatium vinosum*: Structural and Functional Insights into Thiosulfate Oxidation. *Submitted*.

P12-6

## CRYSTAL STRUCTURE ANALYSES OF DIPEPTIDYL PEPTIDASE 11 FROM *PORPHYROMONAS GINGIVALIS*

Y. Sakamoto<sup>1</sup>, Y. Suzuki<sup>2</sup>, I. Iizuka<sup>1</sup>, C. Tateoka<sup>1</sup>, S. Roppongi<sup>1</sup>, M. Fujimoto<sup>1</sup>, K. Inaka<sup>3</sup>, H. Tanaka<sup>4</sup>, M. Yamada<sup>5</sup>, K. Ohta<sup>5</sup>, H. Gouda<sup>6</sup>, T. Nonaka<sup>1</sup>, W. Ogasawara<sup>2</sup>, N. Tanaka<sup>6</sup>

<sup>1</sup>School of Pharmacy, Iwate Medical University, Iwate 028-3694, Japan

<sup>2</sup>Department of Bioengineering, Nagaoka University of Technology, Niigata 940-2188, Japan

<sup>3</sup>Maruwa Foods and Biosciences Inc., Nara 639-1123, Japan

<sup>4</sup>Confocal Science Inc., Tokyo 101-0032, Japan

<sup>5</sup>Japan Aerospace Exploration Agency, Ibaraki 305-8505, Japan

<sup>6</sup>School of Pharmacy, Showa University, Tokyo 142-8555, Japan  
ntanaka@showa-u.ac.jp

Periodontitis is a bacterially induced inflammatory disease that destroys the periodontal tissues, eventually leading to tooth loss. *Porphyromonas gingivalis*, a Gram-negative, anaerobic bacterium, is a major pathogen associated with the chronic form of periodontitis. Because *P. gingivalis* is an asaccharolytic bacterium that gains its metabolic energy by fermenting amino acids, *P. gingivalis* secretes various proteases/peptidases that are capable of digesting external proteins into peptides. *P. gingivalis* utilizes di- and tripeptides, instead of single amino acids, as sources of carbon and energy. Therefore, peptidases of *P. gingivalis* that provide di- and tripeptides are essential for the metabolism of the bacterium, and much attention has been paid to dipeptidyl peptidases (DPPs) from *P. gingivalis*. Recently, novel DPPs, DPP5 (PgDPP5), DPP7 (PgDPP7) and DPP11 (PgDPP11), have been identified from *P. gingivalis* [1-3]. The *P. gingivalis* DPPs, PgDPP5 has been classified as clan SC, family S9 in the MEROPS database, while PgDPP7 and PgDPP11 have been assigned to another type of serine peptidase family, S46 in clan PA. Whereas PgDPP7 exhibits a broad substrate specificity for both

aliphatic and aromatic residues at the P1 position (NH<sub>2</sub>-P2-P1-P1'-P2'-..., where the P1-P1' bond is the scissile bond), PgDPP11 exhibits a strict substrate specificity for acidic residues (Asp/Glu) at the P1 position.

The S46 peptidases are widely distributed in anaerobic Gram-negative species, but they are not found in mammals. Therefore, the family S46 peptidases may represent ideal targets for novel antibiotics. Recently, the first three-dimensional structure of a S46 peptidase was determined for dipeptidyl peptidase BII (DAP BII) from *Pseudoxanthomonas mexicana* WO24 [4]. The study revealed that DAP BII is a homodimer and each subunit contains a peptidase domain including a double  $\beta$ -barrel fold that is characteristic of the chymotrypsin superfamily, as well as an unusual  $\alpha$ -helical domain that regulates the exopeptidase activity of DAP BII. Although the overall structure, the molecular basis of the exopeptidase activity, and the catalytic mechanism of the S46 peptidase have been revealed by the crystal structure analyses of DAP BII [4], determinants for the substrate specificity of S46 peptidases at the atomic level remain to be fully elucidated.

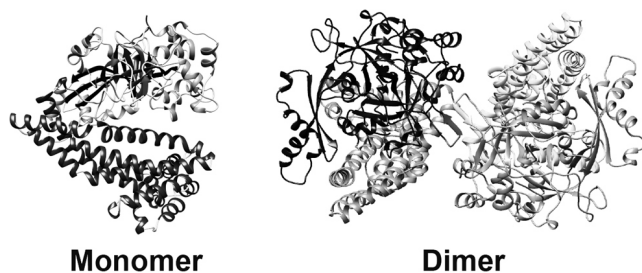


Figure 1. Overall structure of PgDPP11.

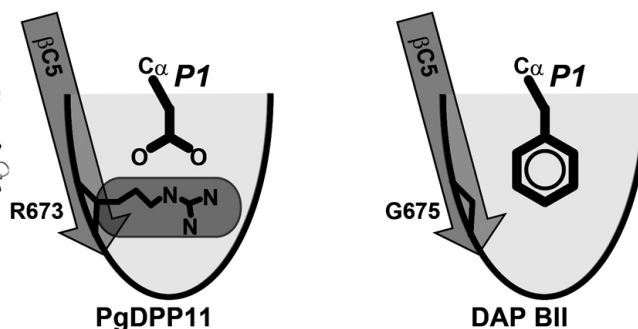


Figure 2. Schematic diagrams of the S1 subsites of S46 peptidases.



In this study, we present the crystal structure of PgDPP11 (Fig. 1), a member of the S46 peptidase family. The crystal structure analyses, *in silico* docking studies, and site-directed mutagenesis studies clearly explain the molecular basis of the Asp/Glu specificity of PgDPP11 [5], which is determined by the conserved Arg residue in the S1 subsite (Fig. 2).

High-resolution diffraction data obtained from a space-grown crystal enabled us to identify two potassium ion-binding sites in the catalytic domain of PgDPP11 because the present crystallisation conditions contained 0.16 M tri-potassium citrate in the reservoir solution. One was found at the N-terminal amino group binding site, and the other was found at the bottom of the S1 subsite. The former potassium ion was coordinated by the side chains of Asn218 and Asp672 and a water molecule and was also stabilised by a cation-pi interaction with the indole ring of Trp219. Similar cation-pi interaction was observed between the indole ring of Trp216 in DAP BII and the N-terminal amino group of bound peptide [4]. The space grown crystal was obtained using a counter-diffusion crystallisation method under a microgravity environment in the Japanese Experimental Module “Kibo” at the International Space Station (ISS) [6].

1. A. Banbula, J. Yen, A. Oleksy, P. Mak, M. Bugno, J. Travis, J. Pogtempa, *J. Biol. Chem.*, **276**, (2001), 6299.
2. Y. Ohara-Nemoto, Y. Shimoyama, S. Kimura, A. Kon, H. Haraga, T. Ono, T. K. Nemoto, *J. Biol. Chem.*, **286**, (2011), 38115.
3. Y. Ohara-Nemoto, S. M. Rouf, M. Naito, A. Yanase, F. Tetsuo, T. Ono, T. Kobayakawa, Y. Shimoyama, S.

Kimura, K. Nakayama, K. Saiki, K. Konishi, T. K. Nemoto, *J. Biol. Chem.*, **289**, (2014), 5436.

4. Y. Sakamoto, Y. Suzuki, I. Iizuka, C. Tateoka, S. Roppongi, M. Fujimoto, K. Inaka, H. Tanaka, M. Masaki, K. Ohta, H. Okada, T. Nonaka, Y. Morikawa, K. T. Nakamura, W. Ogasawara, N. Tanaka, *Sci. Rep.*, **4**, (2014), 4977.
5. Y. Sakamoto, Y. Suzuki, I. Iizuka, C. Tateoka, S. Roppongi, M. Fujimoto, K. Inaka, H. Tanaka, M. Yamada, K. Ohta, H. Gouda, T. Nonaka, W. Ogasawara, N. Tanaka, *Sci. Rep.*, **5**, (2015), 11151.
6. S. Takahashi, K. Ohta, N. Furubayashi, B. Yan, M. Koga, Y. Wada, M. Yamada, K. Inaka, H. Tanaka, H. Miyoshi, T. Kobayashi, S. Kamigaichi, *J. Synchrotron Radiat.*, **20**, (2013), 968.

We thank Drs. Y. Yamada and N. Matsugaki of the Photon Factory and Dr. A. Higashiura, K. Hasegawa and E. Yamashita of SPring-8 for their help with data collection at the synchrotron facilities. This study was supported in part by the Platform for Drug Discovery, Informatics, and Structural Life Science (to N.T.), the Program for the Strategic Research Foundation at Private Universities from the MEXT of Japan (to N.T. and Y.Sa), and a Grant-in-Aid for Scientific Research(C) (to Y.Sa.). This study was also supported in part by “High-Quality Protein Crystal Growth Experiment on JEM” promoted by JAXA (Japan Aerospace Exploration Agency) (to Y.Sa.). The Russian Spacecraft “Progress” and “Soyuz” provided by the Russian Federal Space Agency were used for space transportation.

P12-7

## STRUCTURAL INSIDES INTO SUBSTRATE TUNNELS OF BACTERIAL LIPOXYGENASE FROM *PSEUDOMONAS AERUGINOSA*

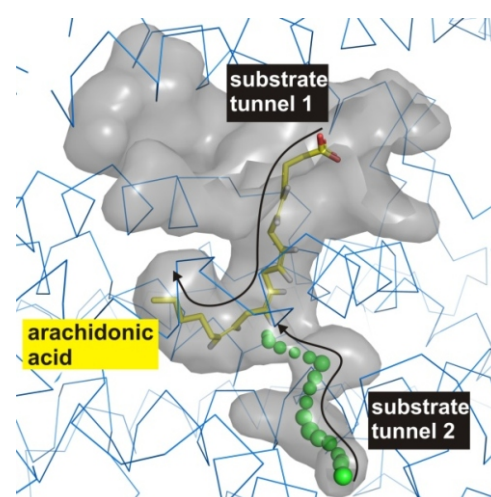
Jacqueline Kalms<sup>1</sup>, Swathi Banthiya<sup>2</sup>, Hartmut Kuhn<sup>2</sup> and Patrick Scheerer<sup>1,\*</sup>

Charité – Universitätsmedizin Berlin, Charitéplatz 1, D-10117 Berlin, Germany

<sup>1</sup>Institut für Medizinische Physik und Biophysik (CC2) - Group Protein X-ray Crystallography and Signal Transduction, <sup>2</sup>Institut für Biochemie (CC2)

\*patrick.scheerer@charite.de

Lipoxygenases are non-heme iron containing enzymes catalyzing the dioxygenation of polyunsaturated fatty acids [1, 2]. The reaction specificity of these enzymes has been used as parameter for their classification. Lipoxygenase of *Pseudomonas aeruginosa* (*PA\_LOX*) oxygenates the substrates arachidonic acid and linoleic acid [3, 4]. After hydrogen abstraction at the active site and rearrangement of a radical, a second substrate, molecular dioxygen, inserts stereospecific, forming a hydroperoxy fatty acid. To make the lipoxygenase reaction possible at the deeply buried active site tunnels for both substrates from the protein surface to the catalytic centre are needed. Two crystal structures of *PA\_LOX* show an active site bound endogenous lipid ligand in a tunnel [4]. To determine the hydrophobic tunnel for molecular dioxygen calculations with the program *Caver* were examined [5]. We found a second tunnel open-



ing leading to the centre of catalysis. Dockings of the substrates arachidonic acid and linoleic acid show the hydrogen involved in the hydrogen abstraction as well as the accessibility to the carbon for oxygen insertion [6].

1. Haeggstrom, J. Z., and Funk, C. D. (2011) Lipoxygenase and leukotriene pathways: biochemistry, biology, and roles in disease. *Chemical reviews* **111**, 5866-5898.
2. Kuhn, H., Banthiya, S., and van Leyen, K. (2015) Mammalian lipoxygenases and their biological relevance. *BBA* **1851**, 308-330.
3. Garreta, A., Val-Moraes, S. P., Garcia-Fernandez, Q., Busquets, M., Juan, C., Oliver, A., Ortiz, A., Gaffney, B. J., Fita, I., Manresa, A., and Carpena, X. (2013) Structure and interaction with phospholipids of a prokaryotic lipoxygenase from *Pseudomonas aeruginosa*. *FASEB journal* **27**, 4811-4821.
4. Banthiya, S. \*, Kalms, J. \*, Yoga E. G., Ivanov, I., Carpena, X., Hamberg, M., Kuhn, H., and Scheerer, P. (2016) Structural and functional basis of phospholipid oxygenase activity of bacterial lipoxygenase from *Pseudomonas aeruginosa*, *submitted*.
5. Eva Chovancová, Antonín Pavelka, Petr Beneš, Ondřej Strnad, Jan Brezovský, Barbora Kozlíková, Artur Gora, Vilém Šustr, Martin Klvaňa, Petr Medek, Lada Biedermannová, Jiří Sochor & Jiří Damborský. (2012) CAVER 3.0: A Tool for the Analysis of Transport Pathways in Dynamic Protein Structures. *PLoS Computational Biology* **8**: e1002708, 8(10).
6. Kalms, J. \*, Banthiya, S. \*, , Yoga E. G. \*, Ivanov, I., Carpena, X., Kuhn, H., and Scheerer, P. (2016) The crystal structure of *Pseudomonas aeruginosa* lipoxygenase Ala420Gly mutant explains its altered reaction specificity, *in preparation*.

P12-8

## CRYSTALLIZATION OF RESURRECTED ANCESTORS OF HALOALKANE DEHALOGENASE DbjA AND DbeA

P. Babková<sup>1</sup>, E. Šebestová<sup>1</sup>, J. Brezovský<sup>1,2</sup>, J. Damborský<sup>1,2</sup>, R. Chaloupková<sup>1,2</sup>

<sup>1</sup> Loschmidt Laboratories, Department of Experimental Biology and Research Centre for Toxic Compounds in the Environment RECETOX, Masaryk University, Kamenice 5/A13, 625 00 Brno, Czech Republic. <sup>2</sup> International Clinical Research Center, St. Anne's University Hospital Brno, Pekarska 53, 656 91 Brno, Czech Republic

Ancestral sequence reconstruction is a powerful approach allowing the resurrection of ancient enzymes based on sequences predicted by a phylogenetic analysis [1]. This paleomolecular approach uncovers the properties of the ancestral proteins, indicating the structural consequences of the molecular evolution [2]. In this project the sequences of representative members of haloalkane dehalogenase subfamily II were selected as targets for prediction of common ancestor of haloalkane dehalogenase DbjA [3-5] and DbeA [6], ancDbjA-DbeA node1, and additional ancestors corresponding to the deeper nodes of the branch leading towards the present-day enzymes, ancDbjA-DbeA node2, ancDbjA-DbeA node3, ancDbjA-DbeA node4 and ancDbjA-DbeA node5. The genes encoding predicted sequences were synthesized; the resurrected proteins were overexpressed in *Escherichia coli* BL21(DE3) cells and purified to homogeneity by metallo-affinity chromatography. All crystallization trials were performed by using the sitting-drop vapor-diffusion method at 23 °C. The crystals of ancDbjA-DbeA node 2, node 3 and node 5 grew during the initial screening and no further optimization of the crystallization conditions was necessary. The triangular prism shaped crystals of ancDbjA-DbeA node3 with dimensions 0.5 x 0.09 x 0.08 mm grew in condition No. 42 of JCSG consisting of 0.02 M magnesium chloride, 0.1 M Tris pH 8.5 and 20% (w/v) PEG 8000. The hexagonally shaped crystals of ancDbjA-DbeA node3 with dimensions 0.2 x 0.1 x 0.04 mm appeared in condition No. 16 of the Wizard classic consisting of 100 mM potassium phosphate/sodium phosphate pH 6.2 and 2.5 M sodium chloride. The trigonal

shaped crystals of ancDbjA-DbeA node5 with average dimension 0.11 x 0.05 x 0.31 mm were observed in condition No. 73 of PEG suite containing 0.2 M magnesium acetate and 20 % (w/v) PEG 3350. These crystals were used for collection of X-ray diffraction data and complete diffraction data sets were collected at 1.66, 1.26 and 1.25 Å resolution for ancDbjA-DbeA node2, ancDbjA-DbeA node3 and ancDbjA-DbeA node 5, respectively. Obtained microcrystals of ancDbjA-DbeA node1 and ancDbjA-DbeA node4 were further optimized by variation of enzyme concentration, pH and precipitant concentration. Optimized crystals of ancDbjA-DbeA node4 appeared within three days from the drop composed of 9.5 % (w/v) mix of PEG 1000, PEG 3350 and MPD, 0.1 M MOPS/HEPES-Na pH 7.0. On-going structural analysis of ancestral enzymes will provide insight into their unique catalytic properties such as high thermodynamic stability and high catalytic activity.

1. Skovgaard M., et al., *J. Mol. Biol.*, 2006, 363, 977-988.
2. Huang R., et al., *Proc. Natl. Acad. Sci.*, 2012, 109, 2966-2971.
3. Sato, Y., et al., *Acta Crystallogr.*, 2007, F63, 294-296.
4. Prokop, Z., et al., *Angew. Chem. Int. Ed. Engl.*, 2010, 49, 6111-6115.
5. Chaloupkova, R., et al., *FEBS J.*, 2011, 278, 2728-2738.
6. Chaloupkova, R., et al., *Acta Crystallogr.*, 2014, D70, 1884-1897.



P12-9

## PROTEIN-LIGAND INTERACTIONS IN HALOALKANE DEHALOGENASES

Michal Kutý<sup>1,2</sup>, David Řeha<sup>1,2</sup>, and Ivana Kuta Smatanova<sup>1,2</sup>

<sup>1</sup>Faculty of Science, University of South Bohemia in Ceske Budejovice, Branisovska 31, 370 05 Ceske Budejovice, Czech Republic

<sup>2</sup>Center for Nanobiology and Structural Biology, Institute of Microbiology of the Academy of Sciences, Czech Republic, 142 20 Prague, Czech Republic  
kutym@seznam.cz

Haloalkane dehalogenases (HLDs) are enzymes that catalyze reactions of great environmental and biotechnological significance. HLDs (EC 3.8.1.5) belong to the  $\alpha$ -hydroxylase superfamily [1] of enzymes catalyzing hydrolytic cleavage of carbon-halogen bonds in halogenated hydrocarbons to yield the corresponding alcohol, a proton and a halide [2]. This work is focused on the protein-ligand interactions in a recently constructed stable and solvent-resistant haloalkane dehalogenase DhaA from *Rhodococcus rhodochrous* NCIMB 13064 and its variants with mutations in the residues that form the access tunnel connecting the enzyme's buried active site to the surrounding solvent. The interactions and different binding sites between a protein and a ligand were studied by using molecular dynamics method GROMACS [3] and PELE [4, 5] (an acronym Protein Energy Landscape Exploration) that combines a Monte Carlo stochastic approach with protein structure prediction and is capable of accurately reproducing long time scale processes.

This research is supported by the GACR (P207/12/0775).

1. Ollis, D. L., Cheah, E., Cygler, M., Dijkstra, B., Frolow, F., Franken, S. M., Harel, M., Remington, S. J., Silman, I., Schrag, J., Sussman, J. L., Verschuere, K. H. G. & Goldman, A. (1992), *Protein Eng.* 5, 197–211.
2. Damborský J., Rorije E., Jesenská A., Nagata Y., Klopman G., Peijnenburg W. J. (2001), *Environ. Toxicol. Chem.*, 20, 2681–2689.
3. Van Der Spoel D, Lindahl E, Hess B, Groenhof G, Mark AE, Berendsen HJ (2005). "GROMACS: fast, flexible, and free". *J Comput Chem* 26 (16): 1701–18.
4. PELE: Protein energy landscape exploration. A novel Monte Carlo based technique (2005), *J. Chem. Theo. Comput.*, 1(6):1304-1311.
5. PELE web server: atomistic study of biomolecular systems at your fingertips (2013), *Nucleic Acids Research*, 41(W1):W322-W328.

P12-10

## MECHANISM AND ENERGETICS OF L-ARGININE BINDING TO ARGININE REPRESSOR PROTEIN IN *E. COLI*

Saurabh Kumar Pandey<sup>1</sup>, David Řeha<sup>1,2</sup>, Milan Melichercik<sup>1,3</sup>, Jannette Carey<sup>4</sup>, Rüdiger Ettrich<sup>1,2</sup>, Babak Minofar<sup>1,2</sup>

<sup>1</sup>Center for Nanobiology and Structural Biology, Academy of Sciences of the Czech Republic, Zamek 136, CZ-373 33 Nove Hrad, Czech Republic

<sup>2</sup>Fac. of Sci., Univ. of South Bohemia, Branišovská 1760, 37005 České Budějovice, Czech Republic

<sup>3</sup>Department of Nuclear Physics and Biophysics, Comenius University, Mlynská dolina F1, 842 48 Bratislava, Slovak Republic

<sup>4</sup>Chemistry Department, Princeton University, Princeton, New Jersey 08544-1009, USA

Arginine repressor protein provides feedback regulation of arginine metabolism upon activation by the negatively cooperative binding of L-arginine. Understanding this phenomenon requires the detailed analysis of each binding event and its effect on global motion of the complex.

Umbrella sampling technique was used to calculate binding energy (potential of mean force) of L-arginines to the ArgRC. Unbinding of L-Arg from ArgR was performed using steered dynamics. Potential of mean force (PMF) was calculated using weighted histogram analysis method in GROMACS. Differently ligated states were prepared either by deleting (from holo-ArgR crystal structure) or adding (to apo-ArgR crystal structure), using YASARA tool.

PMF for holo-5 state was ~12 kcal/mol, while in corresponding apo+1 state it was ~7 kcal/mol. PMF for holo-4 state and apo+2 state were ~4 kcal/mol and ~15 kcal/mol respectively.

The PMF of +1 and -5 states have similar values while that of -4 and +2 states are very different. The huge difference in the PMF between -4 and +2 states could be due to the differently occupied binding pockets in these two systems. Few more repetitions of +2 and -4 states are undergoing, once completed these will hopefully allow us to compare the binding affinity of differently ligated states of ArgRC and their effect on global motion of protein.